

A robust assessment of the local anisotropy of the Hubble constant

Yves-Henri Sanejouand*

Faculté des Sciences et des Techniques, Nantes, France.

December 10th, 2023

Abstract

Magnitude predictions of Λ CDM, as parametrized by the Planck collaboration, are not consistent with the supernova data of the whole Pantheon+ sample even when, in order to take into account the uncertainty about its value, the Hubble constant is adjusted. This is a likely consequence of the increase of the number of low-redshift supernovae in the Pantheon+ sample, with respect to previous such samples. Indeed, when supernovae at redshifts below 0.035 are ignored, Λ CDM predictions become consistent with Pantheon+ data. Interestingly, this is also the case if subsets of low-redshift supernovae roughly centered on the direction of the CMB dipole are considered, together with high-redshift ones. These results seem robust, since they are also obtained with a simple, single-parameter tired-light model.

Keywords: Homogeneity scale, Anisotropy, Supernovae Ia, Luminosity distance, Λ CDM, Linear-coasting models, Tired-light models.

Introduction

Since the seminal work of Einstein [1], most cosmological models have been based upon the hypothesis that the Universe is homogeneous [2, 3]. However, following the discovery that many, then so-called nebulae, are galaxies like our own [4], it has been realized that the neighborhood of the Milky Way is highly structured, with both large voids [5, 6, 7] and superclusters of galaxies [8].

Since, on large scales, the homogeneity ansatz has nowadays been well confirmed [9, 10, 11, 12], a distance threshold above which the observable Universe is indeed nearly homogeneous must exist. This homogeneity scale was found to be around $70 h^{-1}$ Mpc [13, 14, 15], with an upper limit of $260 h^{-1}$ Mpc [16], that is, at a redshift between 0.02 and 0.09. On the other hand, a local anisotropy of the Hubble flow has been noticed [17, 18], which could be a consequence of the way matter is distributed in the vicinity of the Milky Way [19, 20, 21].

In the present study, directions in the sky where the Hubble flow is quiet [22], that is, where Λ CDM predictions are consistent with both low and high-redshift supernova data were looked for. In order to assess the robustness of this analysis, consistency with the predictions of other, non-standard, cosmological models was also considered.

Supernova data

Equatorial coordinates, cosmological (Hubble diagram) redshifts (zHD) and corrected B band magnitudes (mBcorr) of the 1542 supernovae Ia of the Pantheon+ sample [23] were retrieved from the PantheonPlusSh0es page of the github webserver¹. Note that the magnitude of 127 supernovae was measured several times (up to four), for a total of 1700 measurements.

Like in a previous study [11], taking advantage of the large number of data available, the error on magnitude measurements at a given redshift, $\sigma_B(z)$, was estimated using the standard error of the mean, $\overline{m}_B(z)$, of either 10 or 25 magnitude val-

*yves-henri.sanejouand@univ-nantes.fr

¹On april 2023.

ues², of supernovae at a redshift around z .

Note that, in the later case, for the 68 data points thus defined, $\sigma_B(z)$ ranges between 0.015 and 0.15, with a median value of 0.03, that is, 0.1% of the median value of supernova mean magnitudes. Note also that there is a limited number of outliers in the Pantheon+ sample, namely, 89 magnitude values (0.5% of them) more than 1.5 IQR away below the second or above the third quartile for their redshift bin, IQR being the interquartile range.

Mean magnitude values were compared to $m_{th}(z)$, the values predicted by a given cosmological model, using the chi-squared test, that is, by evaluating the likelihood of:

$$\chi_{dof}^2 = \frac{1}{N_{dof}} \sum^{N_{dat}} \epsilon^2(z)$$

where $\epsilon(z)$, the weighted magnitude residual, is:

$$\epsilon(z) = \frac{m_{th}(z) - \overline{m}_B(z)}{\sigma_B(z)} \quad (1)$$

and where N_{dat} is the number of data points considered, N_{dof} being the number of degrees of freedom. In the present study, $N_{dof} = N_{dat} - 1$, since all models considered have a single free parameter, namely, H_0 , the Hubble constant, its value being determined by minimizing χ_{dof}^2 . Remember that χ_{dof}^2 values well above one mean that predictions are not consistent with data. On the other hand, χ_{dof}^2 values well below one usually mean that errors on the data are overestimated.

Predicted magnitudes were obtained as follows:

$$m_{th}(z) = 5 \log_{10}(d_L) + 25 + M \quad (2)$$

where d_L is the luminosity distance, in Mpc, $M = -19.25$ being the fiducial absolute magnitude of supernovae Ia applicable to the Pantheon+ standardization [23].

Cosmological models

Friedmann-Lemaitre models

Within the frame of Friedmann-Lemaitre models, the luminosity distance is given by:

$$d_L = c_0(1+z) \frac{1}{\sqrt{|\Omega_k|}} S_k(\sqrt{|\Omega_k|} \int_0^z \frac{dz'}{H(z')}) \quad (3)$$

²With a minimum of 10 values for the last redshift bin.

where c_0 is the speed of light, Ω_k , the curvature density parameter, and where, when the contribution of the radiation term is neglected:

$$H(z) = H_0 \sqrt{\Omega_m(1+z)^3 + \Omega_k(1+z)^2 + \Omega_\Lambda} \quad (4)$$

Ω_m and Ω_Λ being the matter and cosmological constant density parameters, respectively, while, by definition, $\Omega_m + \Omega_k + \Omega_\Lambda = 1$.

Analyses of Planck measurements of the cosmic microwave background anisotropies are consistent with Λ CDM, that is, a flat ($\Omega_k=0$) Friedmann-Lemaitre model with $\Omega_m = 0.315 \pm 0.007$ [24]. A number of local probes have also been found consistent [25, 26] with this so-called cosmic concordance model [10]. Note however that significant tensions are still under extensive scrutiny [27, 28], noteworthy as far as the value of the Hubble constant is concerned [29]. This is the main reason why, in the present study, it is treated as a free parameter. Note that, in the case of luminosity distances, it would make no difference if the single free parameter were instead the absolute magnitude of supernovae Ia (see eqn 2).

In the second half of last century, the standard cosmological model was the Einstein-de Sitter model, another flat Friedmann-Lemaitre model where $\Omega_m=1$ ($\Omega_\Lambda=0$). In this case, according to eqn 4:

$$H(z) = H_0(1+z)^{3/2}$$

and eqn 3 becomes:

$$d_L = 2 \frac{c_0}{H_0} (1+z - \sqrt{1+z})$$

Recently, linear coasting models [30, 31] have attracted some attention. They are characterized by:

$$H(z) = H_0(1+z)$$

Thus, for a flat model with zero active mass like the $R_h=ct$ one [32, 33], eqn 3 becomes:

$$d_L = \frac{c_0}{H_0} (1+z) \ln(1+z)$$

while, for an open model, like the Dirac-Milne one [34]:

$$d_L = \frac{c_0}{H_0} (1+z) \sinh \{\ln(1+z)\}$$

Tired-light models

Soon after the Hubble-Lemaitre law was revealed [3, 35], alternative explanations were proposed [36, 37]. Noteworthy, the hypothesis that the energy of photons may decay during their travel [38] was backed by a pair of Nobel laureates [39, 40], an exponential law being assumed, likely by analogy with radioactive processes, namely:

$$h\nu_{obs} = h\nu_0 e^{-\frac{H_0}{c_0} d_T}$$

where ν_0 and ν_{obs} are, respectively, the frequency of the photons when they are emitted and when they are observed at d_T , the light-travel distance from their source, h being the Planck constant. As a consequence:

$$d_L = \frac{c_0}{H_0} \sqrt{1+z} \ln(1+z)$$

This model is hereafter coined eTL, standing for the exponential tired-light model.

Another tired-light model backed by a Nobel laureate [41] just assumes that the Hubble law has a general character [42, 43], namely, that:

$$d_T = \frac{c_0}{H_0} z$$

Thus:

$$d_L = \frac{c_0}{H_0} z \sqrt{1+z}$$

This model is hereafter coined lTL, standing for the linear tired-light model.

All models above assume that the Universe is transparent enough, so that absorption, noteworthy by grey dust [44, 45], can be safely neglected. So, let us also consider a more recent, non conservative tired-light model [11], hereafter coined ncTL, where, traveling on cosmological distances, photons are assumed to have significant chances to be lost, in such a way that:

$$n_{obs} = n_0 e^{-\sigma_o N_o d_T} \quad (5)$$

where n_0 and n_{obs} are, respectively, the number of emitted photons and the number of photons that can be observed at a distance d_T from their source, σ_o and N_o being respectively the average cross-section and number density of obstacles.

On the other hand, assuming that, at least in the single-photon regime, the energy lost by a given

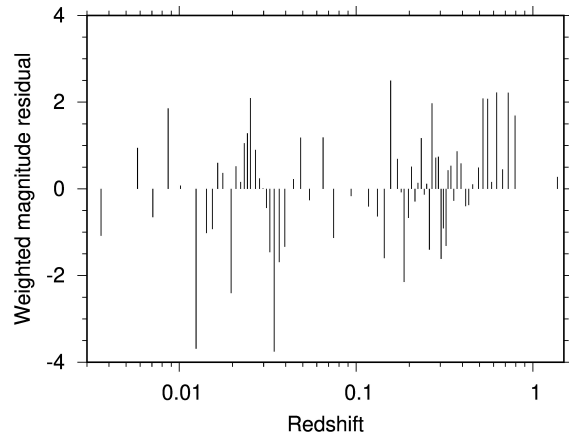


Figure 1: Difference between the magnitude predicted by Λ CDM and the mean observed one, in units of the standard error of the mean magnitude of the supernovae, as a function of redshift. For each of the 68 redshift bins, 25 magnitude values are considered.

photon is proportional to the surface of the wavefront associated to this photon [46, 47] that has crossed an obstacle during the travel of the photon between the source and the observer yields:

$$h\nu_{obs} = h\nu_0 \left(1 - \frac{N_{tot}\sigma_o}{4\pi d_T^2}\right)$$

where N_{tot} is the total number of obstacles crossed by the wavefront. Thus:

$$\frac{z}{1+z} = \frac{1}{3} \sigma_o N_o d_T \quad (6)$$

which, if it is assumed that:

$$H_0 = \frac{1}{3} c_0 \sigma_o N_o$$

is a Hubble-like law previously shown to be consistent with observational data of various origins [11, 48]. Thus, with eqn 5 and 6:

$$d_L = \frac{c_0}{H_0} \frac{z}{\sqrt{1+z}} e^{\frac{3}{2} \frac{z}{1+z}}$$

Results

Local inhomogeneity

When supernova mean magnitudes over the whole redshift range (0.004–1.38) are considered, predic-

Table 1: Consistency of seven cosmological models with the supernova data of the Pantheon+ sample, when supernovae at redshifts below 0.05 are ignored. For each model, H_0 is adjusted so as to minimize χ_{dof}^2 . Top: Friedman-Lemaitre models. Bottom: Tired-light models.

| Model | H_0 (km/s/Mpc) | χ_{dof}^2 | p-value |
|-------------------|---------------------|----------------|---------|
| Λ CDM | 73.4 | 1.29 | 0.08 |
| Dirac-Milne | 70.3 | 1.55 | 0.01 |
| $R_h=ct$ | 69.3 | 2.21 | 0.00001 |
| Einstein-deSitter | 64.7 | 12.3 | 0^a |
| ncTL | 75.1 | 1.23 | 0.12 |
| lTL | 69.6 | 1.85 | 0.0005 |
| eTL | 60.4 | 34.8 | 0^b |

^a 10^{-83} ; ^b 10^{-279} .

tions of Λ CDM are not found consistent with them ($\chi_{dof}^2 = 1.70$, p-value = 3.10^{-4}). As shown in Figure 1, $\epsilon(z)$, the weighted magnitude residual (eqn 1), has large absolute values, noteworthy around 4 for a pair of data points at $z=0.012$ and 0.034 .

On the other hand, as shown in Table 1, when supernovae at redshifts below 0.05 are ignored, while most models considered in the present study still do not prove able to match the supernova data (p-value $\ll 0.05$), a pair of them are standing out, namely, Λ CDM and ncTL.

In the former case, note that the value of the Hubble constant for which χ_{dof}^2 is minimum ($H_0 = 73.4 \text{ km}\cdot\text{s}^{-1}\cdot\text{Mpc}^{-1}$) is in perfect agreement with the latest measurement of the SH0ES team ($H_0 = 73.0 \pm 1.0 \text{ km}\cdot\text{s}^{-1}\cdot\text{Mpc}^{-1}$) [49].

Low-redshift threshold

As shown in Figure 2, Λ CDM predictions become consistent with the data from the Pantheon+ sample when only supernovae at redshifts above a threshold of 0.034 are considered. Note that this threshold corresponds to the second high-value weighted magnitude residual mentioned above.

Interestingly, ncTL predictions become also consistent with supernova data above approximately the same threshold (Fig. 2), even though they are poorer when the whole Pantheon+ sample is considered ($\chi_{dof}^2 = 2.49$, p-value = 2.10^{-10}).

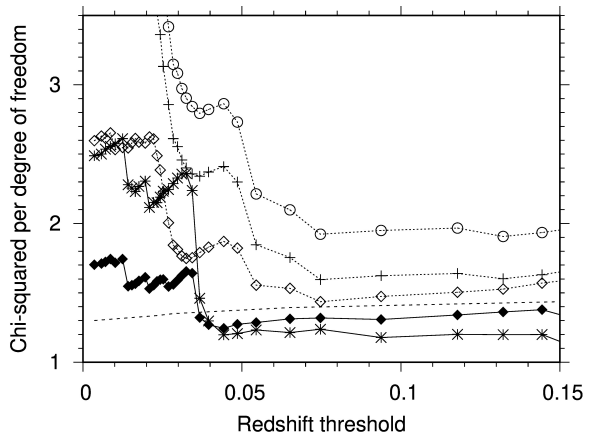


Figure 2: Chi-squared per degree of freedom as a function of the lowest supernova redshift taken into account. The dashed line indicates the value of χ_{dof}^2 below which model predictions are consistent with supernova mean magnitudes (p-value=0.05). Filled diamonds: Λ CDM; open circles: $R_h=ct$; open diamonds: Dirac-Milne; pluses: lTL; stars: ncTL. Being all over 3.5, χ_{dof}^2 values for the Einstein-de Sitter and eTL models are not shown.

Taken together, these results suggest that model predictions can only become consistent with the Pantheon+ data above a specific scale, which is likely to be the homogeneity one. They also illustrate the main reason why supernovae at redshifts below 0.02–0.03 are nowadays not taken into account when accurate measurements of the Hubble constant are performed [49, 50, 51].

Note that, with a redshift threshold of 0.16, predictions of the $R_h=ct$, Dirac-Milne and lTL models are also found consistent with supernova data, as claimed in the case of the two former in previous studies performed with smaller samples [34, 52].

Sky maps

Since the value of the Hubble constant seems to vary from a direction in the sky to the other [53, 54] and since a dipole in the Pantheon+ data is not detected any more when supernovae at redshifts below 0.05 are ignored [55], directions in the sky along which the Hubble constant is the same at low and high-redshifts were looked for, as follows.

First, all 42 high-redshift ($z \geq 0.05$) data points considered above were kept. Second, for each of

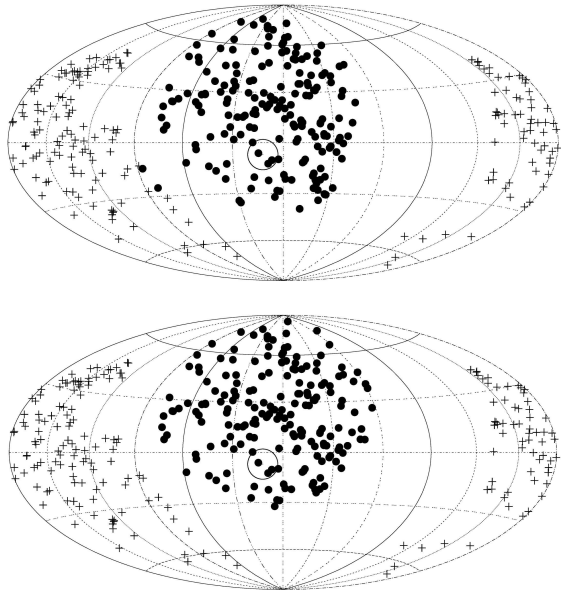


Figure 3: Location in the sky of the subsets of low-redshift supernovae whose magnitudes are the more (filled circles) or the less (crosses) consistent with both the magnitudes of high-redshift supernovae and the predictions of Λ CDM (top) or ncTL (bottom). Open circles: the direction of the CMB dipole. Hammer projections of equatorial coordinates.

the 478 low-redshift ($z < 0.05$) supernovae of the Pantheon+ sample, the 260 magnitudes of the low-redshift supernovae that are the closest on the sky were also taken into account, with 10 magnitude values per redshift bin, so as to have, for each data set, as many points as above, with the whole Pantheon+ sample, namely, 68.

Predictions of Λ CDM and ncTL are not consistent with most of these 478 data sets, the average χ^2_{dof} being 1.47 ± 0.01 (p-value = 7.10^{-3}) and 1.78 ± 0.01 (p-value = 9.10^{-5}), respectively. However, they are found consistent (p-value ≥ 0.05) with 124 (26%) and 48 (10%) of them, respectively.

Interestingly, as shown in Figure 3, the low-redshift supernova datasets that are the more, or the less, consistent with both high-redshift data and either Λ CDM or ncTL largely overlap. As a matter of fact, they are almost identical. For Λ CDM, the best fit ($\chi^2_{dof} = 1.05$; p-value=0.37) is obtained with the closest low-redshift neighbors

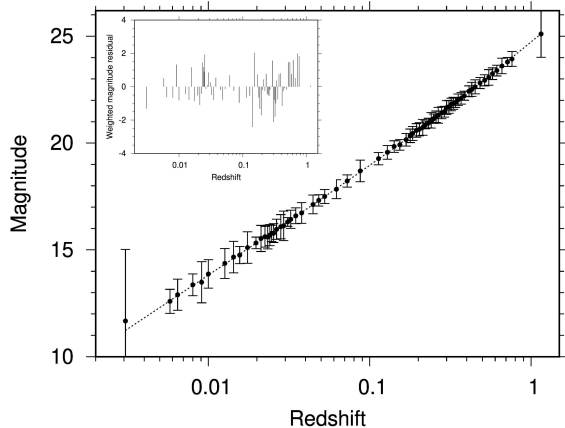


Figure 4: Mean magnitude of the supernovae Ia of the Pantheon+ sample, as a function of redshift. Dotted line: as predicted by Λ CDM. For $z \geq 0.05$, each of the 42 data points (filled circles) is an average over 25 supernova magnitudes. For $z < 0.05$, it is an average over 10 ones, the 260 selected values being the magnitudes of the supernovae the closest in the sky to 2016afk. Error bars are showing the corresponding standard errors, multiplied by ten for the sake of clarity. Inset: weighted magnitude residuals.

(Fig. 3, top) of supernova 2016afk ($\alpha = 155.6^\circ$, $\delta = 15.1^\circ$) while, for ncTL, it is obtained ($\chi^2_{dof} = 1.10$; p-value=0.27) with the closest low-redshift neighbors (Fig. 3, bottom) of supernova ASASSN-16db ($\alpha = 167.4^\circ$, $\delta = 29.6^\circ$). Interestingly, the direction of the CMB dipole ($\alpha = 168^\circ$, $\delta = -7^\circ$ [56]) belongs to the area of the sky covered by both sets of supernovae, in line with recent results showing that H_0 is larger in an hemisphere encompassing this direction [57].

On the other hand, the value of the Hubble constant for which χ^2_{dof} is minimum is $73.4 \text{ km}\cdot\text{s}^{-1}\cdot\text{Mpc}^{-1}$, for Λ CDM, and $74.9 \text{ km}\cdot\text{s}^{-1}\cdot\text{Mpc}^{-1}$, for ncTL, that is, close to values obtained when low-redshift data are ignored (see Table 1).

Figure 4 shows the best fit over the whole redshift range thus obtained with Λ CDM. As expected, weighted magnitude residuals have been downsized, none of them being over 2.4.

Conclusion

Λ CDM predictions become consistent with the Pantheon+ data when supernovae at redshifts below 0.035 are ignored (Fig. 2), suggesting that over this threshold the homogeneity ansatz can be assumed safely. This redshift threshold corresponds to an homogeneity scale of $100 h^{-1}$ Mpc, significantly above most previous estimates [13, 14, 15], but well below upper limits [16].

Λ CDM predictions become also consistent with both low and high redshift supernova data when low redshift ones come from an area of the sky whose center is roughly 30° above the direction of the CMB (Fig. 3). This means that, in this direction, the Hubble flow is quiet, down to $z \approx 0.006$, at least (Fig. 4).

Both results seem robust since they are also obtained with a single free parameter tired light model which, interestingly, happens to be more sensitive to local inhomogeneities (Fig. 2).

References

- [1] Einstein, A. (1917). Kosmologische betrachtungen zur allgemeinen Relativitätstheorie. *Sitz. Preuss. Akad. Wiss.* **1**, 142–152.
- [2] Friedman, A. (1922). Über die krümmung des raumes. *Zeitschrift für Physik* **10**(1), 377–386.
- [3] Lemaitre, G. (1927). Un Univers homogène de masse constante et de rayon croissant rendant compte de la vitesse radiale des nébuleuses extra-galactiques. *Ann. Soc. Sci. Bruxelles* **47**, 49–59.
- [4] Hubble, E.P. (1926). A spiral nebula as a stellar system: Messier 33. *Astrophysical Journal*, *63*, 236-274 (1926) **63**.
- [5] Zehavi, I., Riess, A.G., Kirshner, R.P. & Dekel, A. (1998). A local Hubble bubble from type Ia supernovae ? *Ap. J.* **503**(2), 483.
- [6] Tully, R.B., Shaya, E.J., Karachentsev, I.D., Courtois, H.M., Kocevski, D.D., Rizzi, L. & Peel, A. (2008). Our peculiar motion away from the local void. *Ap. J.* **676**(1), 184.
- [7] Keenan, R.C., Barger, A.J. & Cowie, L.L. (2013). Evidence for a ≈ 300 megaparsec scale under-density in the local galaxy distribution. *Ap. J.* **775**(1), 62.
- [8] Tully, R.B., Courtois, H., Hoffman, Y. & Pomarède, D. (2014). The Laniakea supercluster of galaxies . *Nature* **513**(7516), 71–73.
- [9] Penzias, A.A. & Wilson, R.W. (1965). A measurement of excess antenna temperature at 4080 mc/s. *Ap. J.* **142**, 419–421.
- [10] Tegmark, M., Zaldarriaga, M. & Hamilton, A.J. (2001). Towards a refined cosmic concordance model: Joint 11-parameter constraints from the cosmic microwave background and large-scale structure. *Phys. Rev. D* **63**(4), 043007.
- [11] Sanejouand, Y.H. (2022). A framework for the next generation of stationary cosmological models. *Int. J. Mod. Phys. D* **31**(31), 2250084.
- [12] Aluri, P.K., Cea, P., Chingangbam, P., Chu, M.C., Clowes, R.G., Hutsemékers, D., Kochappan, J.P., Lopez, A.M., Liu, L., Martens, N.C. *et al.* (2023). Is the observable universe consistent with the cosmological principle? *Classical Quantum Gravity* **40**(9), 094001.
- [13] Hogg, D.W., Eisenstein, D.J., Blanton, M.R., Bahcall, N.A., Brinkmann, J., Gunn, J.E. & Schneider, D.P. (2005). Cosmic homogeneity demonstrated with luminous red galaxies. *Ap. J.* **624**(1), 54.
- [14] Sarkar, P., Yadav, J., Pandey, B. & Bhadravaj, S. (2009). The scale of homogeneity of the galaxy distribution in SDSS DR6. *Mon. Not. R. Astron. Soc. Lett.* **399**(1), L128–L131.
- [15] Ntelis, P., Hamilton, J.C., Le Goff, J.M., Burtin, E., Laurent, P., Rich, J., Tinker, J., Aubourg, E., Des Bourboux, H.D.M., Bautista, J. *et al.* (2017). Exploring cosmic homogeneity with the BOSS DR12 galaxy sample. *J. Cosmol. Astrop. Phys.* **2017**(06), 019.
- [16] Yadav, J.K., Bagla, J. & Khandai, N. (2010). Fractal dimension as a measure of the scale of homogeneity. *Mon. Not. R. Astron. Soc.* **405**(3), 2009–2015.

- [17] Davis, M. & Peebles, P. (1983). Evidence for local anisotropy of the Hubble flow. *Annual Review of Astronomy and Astrophysics* **21**(1), 109–130.
- [18] Bolejko, K., Nazer, M.A. & Wiltshire, D.L. (2016). Differential cosmic expansion and the Hubble flow anisotropy. *J. Cosmol. Astrop. Phys.* **2016**(06), 035.
- [19] Buchert, T., Kerscher, M. & Sicka, C. (2000). Back reaction of inhomogeneities on the expansion: The evolution of cosmological parameters. *Phys. Rev. D* **62**(4), 043525.
- [20] Enqvist, K. & Mattsson, T. (2007). The effect of inhomogeneous expansion on the supernova observations. *J. Cosmol. Astrop. Phys.* **2007**(02), 019.
- [21] Heinesen, A. & Macpherson, H.J. (2022). A prediction for anisotropies in the nearby Hubble flow. *J. Cosmol. Astrop. Phys.* **2022**(03), 057.
- [22] Ekholm, T., Baryshev, Y., Teerikorpi, P., Hanski, M. & Paturel, G. (2001). On the quiescence of the Hubble flow in the vicinity of the Local Group-A study using galaxies with distances from the Cepheid PL-relation. *Astronomy & Astrophysics* **368**(3), L17–L20.
- [23] Scolnic, D., Brout, D., Carr, A., Riess, A.G., Davis, T.M., Dwomoh, A., Jones, D.O., Ali, N., Charvu, P., Chen, R. *et al.* (2022). The Pantheon+ analysis: the full data set and light-curve release. *Ap. J.* **938**(2), 113.
- [24] Aghanim, N., Akrami, Y., Ashdown, M., Aumont, J., Baccigalupi, C., Ballardini, M., Banday, A., Barreiro, R., Bartolo, N., Basak, S. *et al.* (2020). Planck 2018 results. VI. Cosmological parameters. *Astronomy & Astrophysics* **641**, A6.
- [25] Cao, S., Ryan, J. & Ratra, B. (2021). Using Pantheon and DES supernova, baryon acoustic oscillation, and Hubble parameter data to constrain the Hubble constant, dark energy dynamics, and spatial curvature. *Mon. Not. R. Astron. Soc.* **504**(1), 300–310.
- [26] Cao, S. & Ratra, B. (2022). Using lower redshift, non-CMB, data to constrain the Hubble constant and other cosmological parameters. *Mon. Not. R. Astron. Soc.* **513**(4), 5686–5700.
- [27] Di Valentino, E., Mena, O., Pan, S., Visinelli, L., Yang, W., Melchiorri, A., Mota, D.F., Riess, A.G. & Silk, J. (2021). In the Realm of the Hubble tension – a review of solutions. *Classical Quantum Gravity* **38**, 152001.
- [28] Nunes, R.C. & Vagnozzi, S. (2021). Arbitrating the s8 discrepancy with growth rate measurements from redshift-space distortions. *Mon. Not. R. Astron. Soc.* **505**(4), 5427–5437.
- [29] Wong, K.C., Suyu, S.H., Chen, G.C., Rusu, C.E., Millon, M., Sluse, D., Bonvin, V., Fassnacht, C.D., Taubenberger, S., Auger, M.W. *et al.* (2020). H0LiCOW XIII. A 2.4% measurement of H0 from lensed quasars: 5.3 σ tension between early and late-Universe probes. *Mon. Not. R. Astron. Soc.* **498**, 1420–1439.
- [30] Kolb, E.W. (1989). A coasting cosmology. *Ap. J.* **344**, 543–550.
- [31] Kaplinghat, M., Steigman, G., Tkachev, I. & Walker, T. (1999). Observational constraints on power-law cosmologies. *Phys. Rev. D* **59**(4), 043514.
- [32] Melia, F. & Shevchuk, A.S.H. (2012). The $R_h = ct$ universe. *Month. Not. Roy. Astron. Soc.* **419**(3), 2579–2586.
- [33] Melia, F. & Maier, R.S. (2013). Cosmic chronometers in the $R_h = ct$ Universe. *Month. Not. Roy. Astron. Soc.* **432**(4), 2669–2675.
- [34] Benoit-Lévy, A. & Chardin, G. (2012). Introducing the Dirac-Milne universe. *A&A* **537**, A78.
- [35] Hubble, E. (1929). A relation between distance and radial velocity among extra-galactic nebulae. *Proc. Natl. Acad. Sc. USA* **15**(3), 168–173.
- [36] Zwicky, F. (1929). On the redshift of spectral lines through interstellar space. *Proc. Nat. Acad. Sc. USA* **15**(10), 773–779.

- [37] North, J.D. (1965). *The measure of the universe. A History of modern cosmology*. Oxford University Press.
- [38] Stewart, J.Q. (1931). Nebular red shift and universal constants. *Phys. Rev.* **38**(11), 2071.
- [39] Nernst, W. (1937). Weitere prüfung der annahme eines stationären zustandes im weltall. *Zeitschrift für Physik* **106**(9-10), 633–661.
- [40] de Broglie, L. (1966). Sur le déplacement des raies émises par un objet astronomique lointain. *Comptes Rendus Acad. Sci. Paris* **263**, 589–592.
- [41] Born, M. (1954). On the interpretation of Freundlich’s red-shift formula. *Proc. Phys. Soc. A* **67**(2), 193.
- [42] Finlay-Freundlich, E. (1954). Red-shifts in the spectra of celestial bodies. *Proc. Phys. Soc. A* **67**(2), 192.
- [43] Lerner, E.J., Falomo, R. & Scarpa, R. (2014). UV surface brightness of galaxies from the local Universe to $z \approx 5$. *Int. J. Mod. Phys. D* **23**, 1450058.
- [44] Simonsen, J.T. & Hannestad, S. (1999). Can dust segregation mimic a cosmological constant? *Astron. Astrophys.* **351**(1), 1–9.
- [45] Robaina, A.R. & Cepa, J. (2007). Redshift-distance relations from type Ia supernova observations—New constraints on grey dust models. *Astron. Astrophys.* **464**(2), 465–470.
- [46] de Broglie, L. (1987). Interpretation of quantum mechanics by the double solution theory. *Ann. Fond. de Broglie* **12**, pages 1–23.
- [47] Jacques, V., Wu, E., Toury, T., Treussart, F., Aspect, A., Grangier, P. & Roch, J.F. (2005). Single-photon wavefront-splitting interference: an illustration of the light quantum in action. *The European Physical Journal D-Atomic, Molecular, Optical and Plasma Physics* **35**, 561–565.
- [48] Sanejouand, Y.H. (2014). A simple Hubble-like law in lieu of dark energy. *arXiv* **1401**, 2919.
- [49] Riess, A.G., Yuan, W., Macri, L.M., Scolnic, D., Brout, D., Casertano, S., Jones, D.O., Murakami, Y., Anand, G.S., Breuval, L. *et al.* (2022). A comprehensive measurement of the local value of the Hubble constant with 1 km s⁻¹ Mpc⁻¹ uncertainty from the Hubble Space Telescope and the SH0ES team. *Ap. J. letters* **934**(1), L7.
- [50] Camarena, D. & Marra, V. (2020). Local determination of the Hubble constant and the deceleration parameter. *Physical Review Research* **2**(1), 013028.
- [51] Popovic, B., Brout, D., Kessler, R. & Scolnic, D. (2023). The Pantheon+ Analysis: Forward Modeling the Dust and Intrinsic Color Distributions of Type Ia Supernovae, and Quantifying Their Impact on Cosmological Inferences. *Ap. J.* **945**(1), 84.
- [52] Wei, J.J., Wu, X.F., Melia, F. & Maier, R.S. (2015). A comparative analysis of the supernova legacy survey sample with Λ CDM and the Rh=ct universe. *A. J.* **149**(3), 102.
- [53] McClure, M.L. & Dyer, C. (2007). Anisotropy in the Hubble constant as observed in the HST extragalactic distance scale key project results. *New Astronomy* **12**(7), 533–543.
- [54] Zhai, Z. & Percival, W.J. (2022). Sample variance for supernovae distance measurements and the Hubble tension. *Phys. Rev. D* **106**(10), 103527.
- [55] Sorrenti, F., Durrer, R. & Kunz, M. (2023). The Dipole of the Pantheon+ SH0ES Data. *J. Cosmol. Astrop. Phys.* **2023**(11), 054.
- [56] Hinshaw, G., Weiland, J., Hill, R., Odegard, N., Larson, D., Bennett, C., Dunkley, J., Gold, B., Greason, M., Jarosik, N. *et al.* (2009). Five-year wilkinson microwave anisotropy probe* observations: data processing, sky maps, and basic results. *The Astrophysical Journal Supplement Series* **180**(2), 225.
- [57] Krishnan, C., Mohayaee, R., Colgáin, E.Ó., Sheikh-Jabbari, M. & Yin, L. (2022). Hints of FLRW breakdown from supernovae. *Phys. Rev. D* **105**(6), 063514.